

## Self-limiting thin film deposition of amorphous metal oxides from aprotic solvents for oxygen evolution electrocatalysis: advancing energy storage and conversion technologies

Rafael A. Prato M.,<sup>a,b</sup> Jan Fransaer,<sup>b</sup> and Xochitl Dominguez-Benetton<sup>a</sup>

### Electronic Supplementary Information

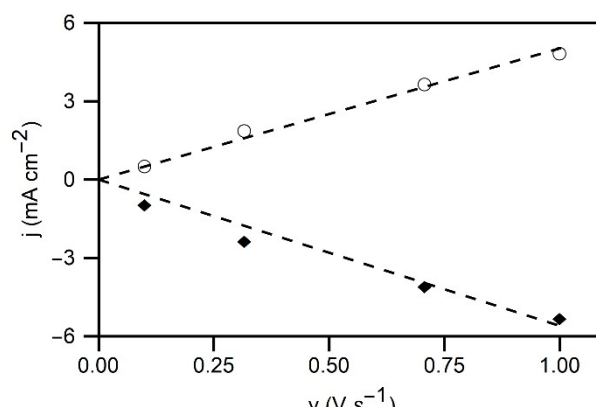


Figure S1. Peak current density for the reduction and oxidation peaks of the pseudoreversible ORR on glassy carbon electrodes in 0.1 M TBAC in DMF.

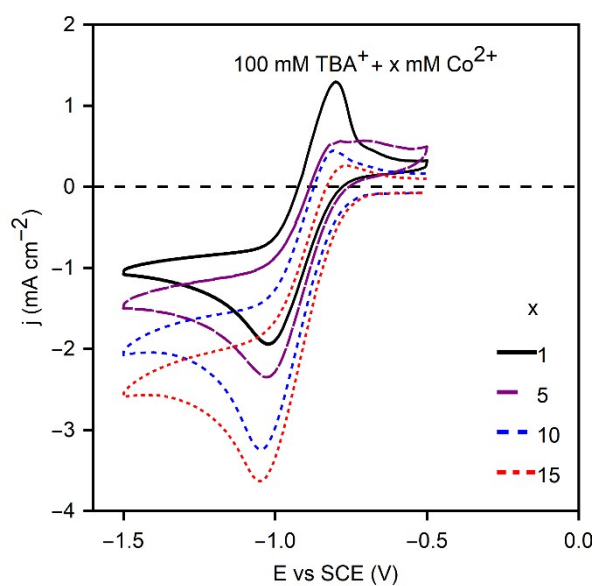


Figure S2. Current density vs potential cycles of a glassy carbon electrode in DMF saturated with oxygen with 0.1 M of TBAC and increasing concentrations of  $\text{CoCl}_2$ : 1 mM, 5 mM, 10 mM and 15 mM, at a scan rates of  $1000 \text{ mV s}^{-1}$ .

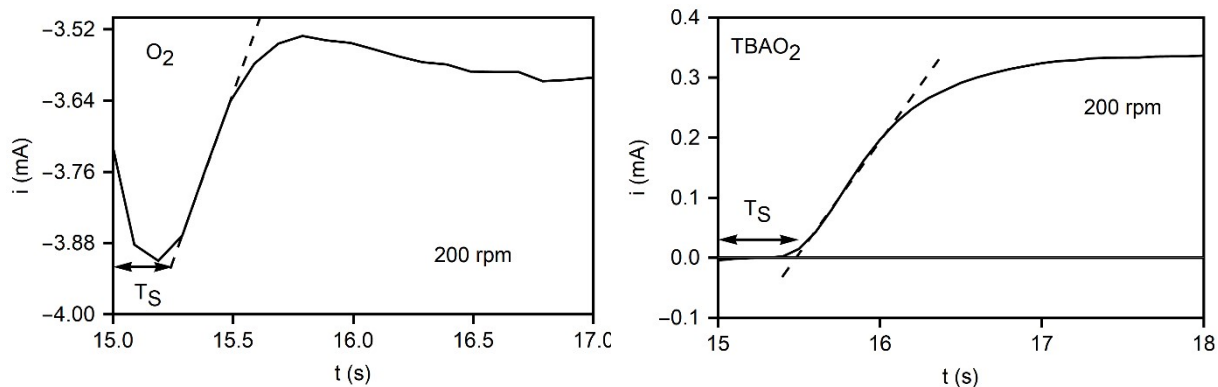


Figure S3. Transient time experiments performed at the rotating ring disk electrode in 0.1 M TBAC in DMF. The ring potential was fixed at -1.2 V vs SCE (left) or +0.2 V vs SCE (right), after 15 seconds the disk potential is stepped to -1.2 V vs SCE.

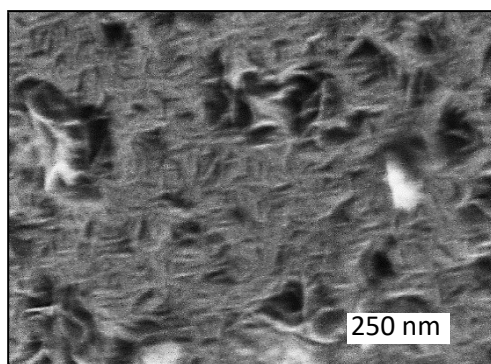


Figure S4. Nano-SEM micrograph of the surface of a  $\text{CoO}_x$  film deposited from 20 cycles, the scale bar shown is 250 nm

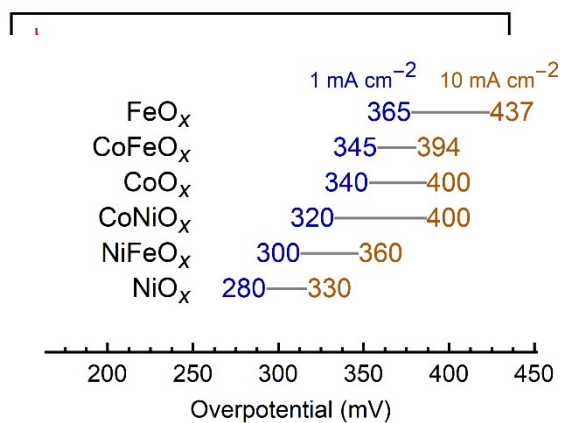


Figure S5. XRD traces from a Co source ( $K\alpha = 1.79 \text{ \AA}$ ) of a glassy carbon plate (GC, black) and a  $\text{NiO}_x$  coated glassy carbon plate ( $\text{NiO}_x/\text{GC}$ , red)

**b**

Figure S6.  $1 \text{ mA cm}^{-2}$  and  $10 \text{ mA cm}^{-2}$  overpotentials for all the studied oxides films deposited from 20 cycles.

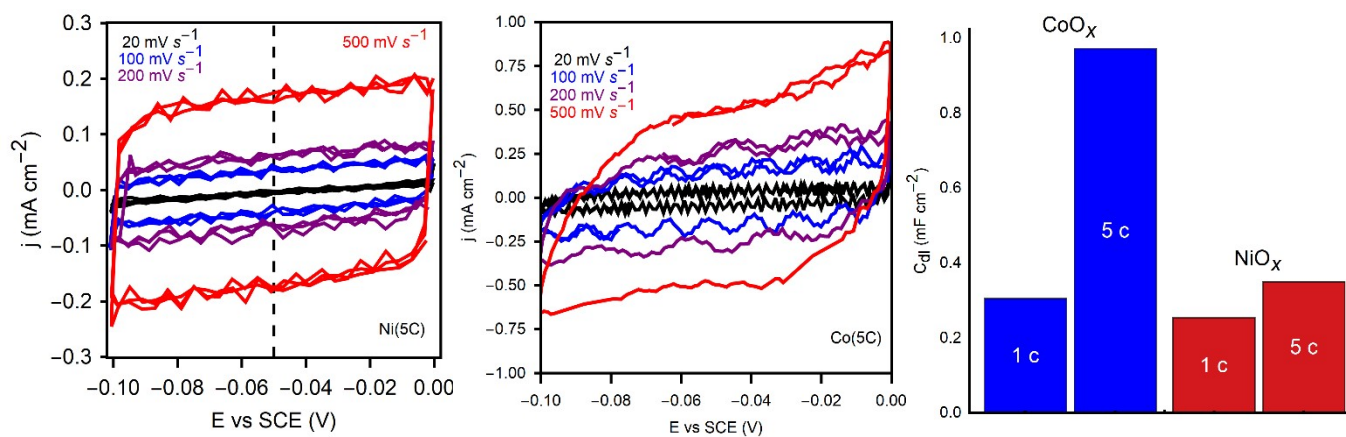


Figure S7. CVs in the non-faradaic region for films deposited with 5 cycles in (left) NiCl<sub>2</sub> and (right) CoCl<sub>2</sub>. Right: double layer capacitance of 1 cycle (1c) and 5 cycle (5c) depositions of NiO<sub>x</sub> and CoO<sub>x</sub> films

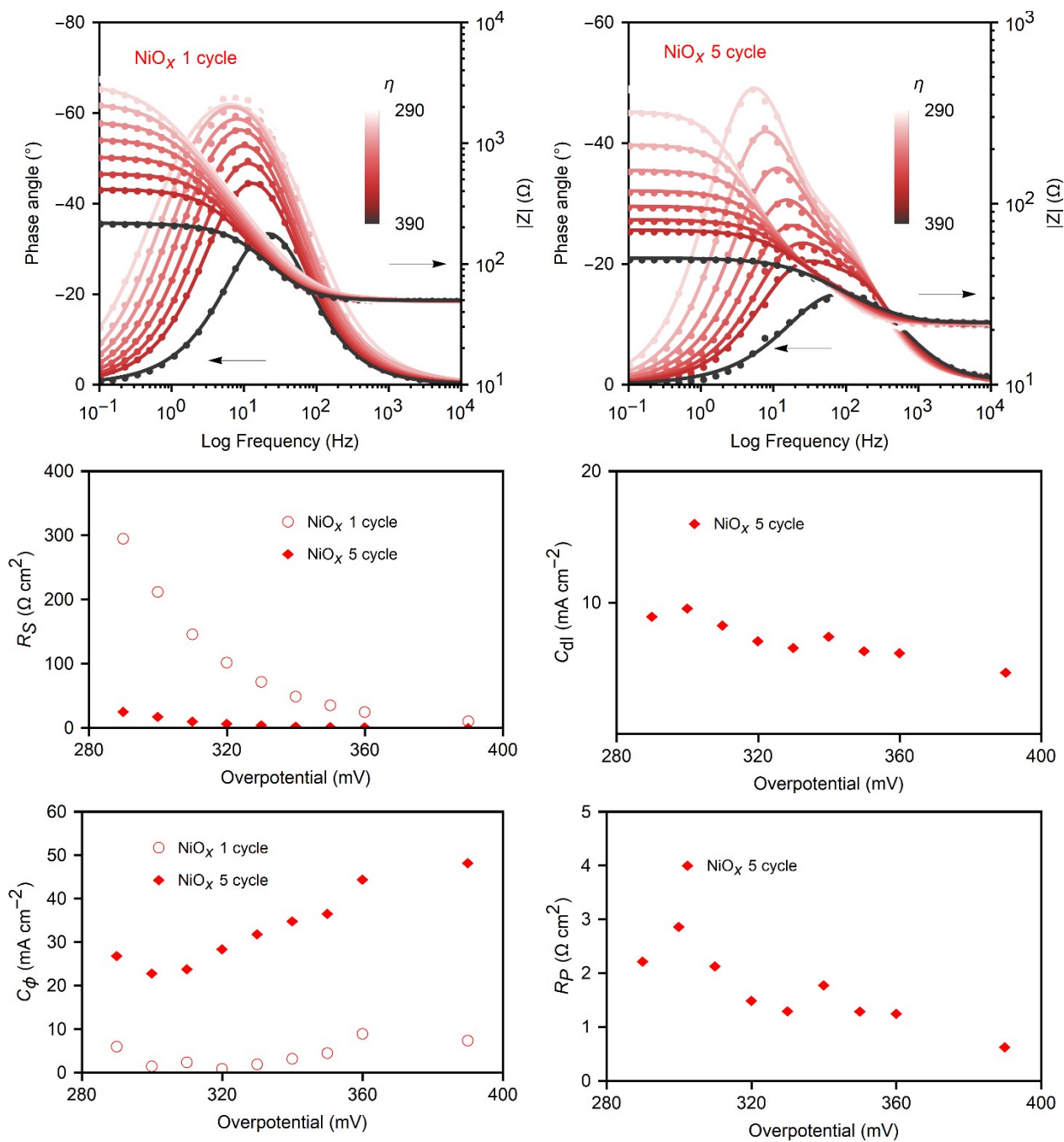
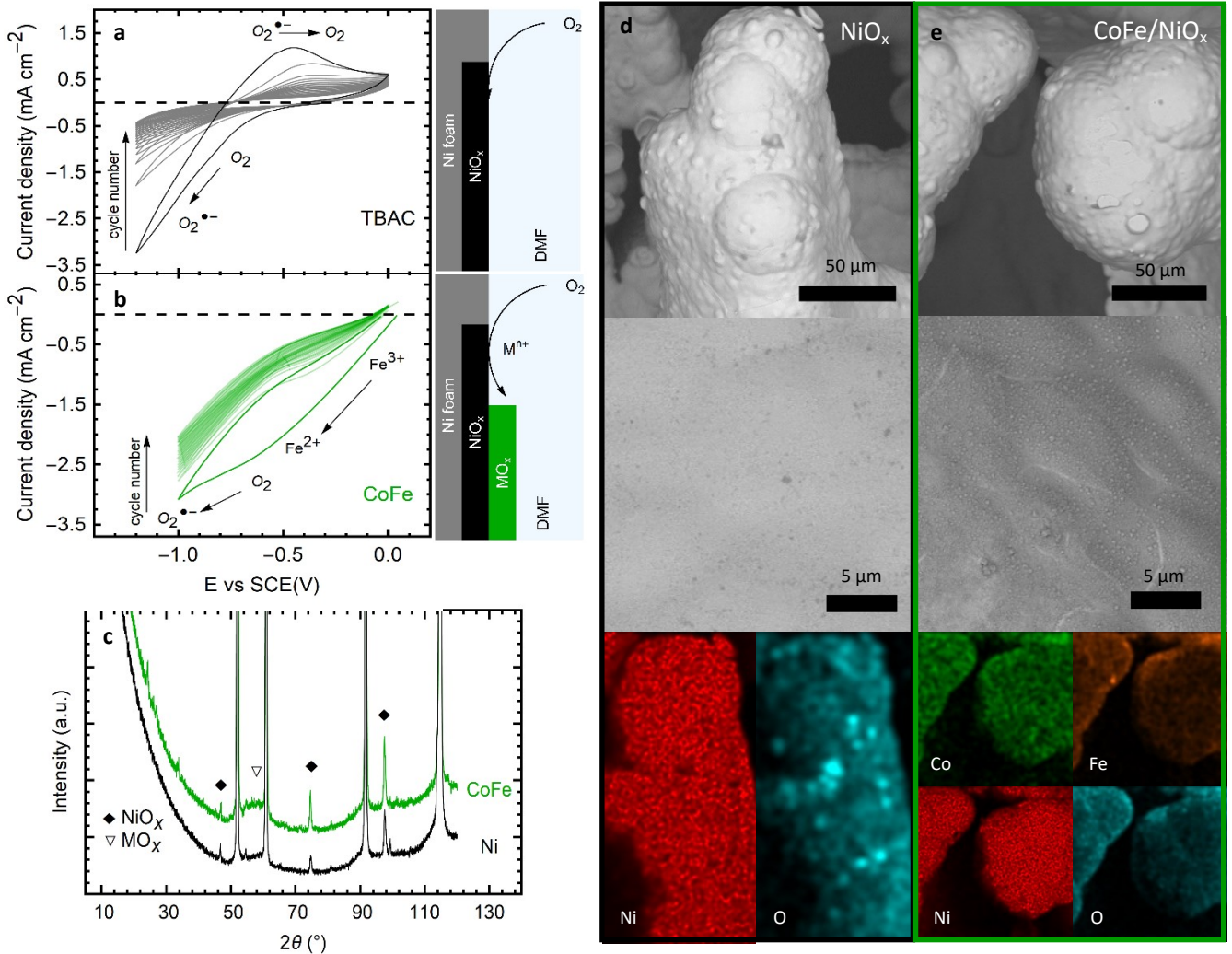


Figure S8. Equivalent circuit model (top). Bode plots showing the impedance magnitude and phase shift of the nickel oxide films deposited from 1 and 5 deposition cycles. The relevant fitted parameters are shown below.



**Figure S9.** Current density vs potential cycles of NF in DMF with: **a)** 0.1 M TBAC, saturated with oxygen, at a scan rate of 50 mV s<sup>-1</sup> **b)** 0.05 M CoCl<sub>2</sub> and 0.05 M FeCl<sub>2</sub> saturated with oxygen, at 50 mV s<sup>-1</sup>. Sketches of the respective processes accompany the curves. **c)** Diffractograms of Ni foam electrodes cycled in TBAC (black, Ni) or in CoCl<sub>2</sub> + FeCl<sub>2</sub> electrolyte (Green, CoFe). Highest intensity peaks correspond to metallic Ni, smaller peaks are annotated. SEM images from backscattered electrons of nickel foam first cycled 20 times in DMF solutions of (column **d**) TBAC and (column **e**) CoCl<sub>2</sub> + FeCl<sub>2</sub> and then cycled 20 times in 3 M KOH/H<sub>2</sub>O for the OER tests. Bottom: EDX elemental mapping of the constituent metals, and oxygen.

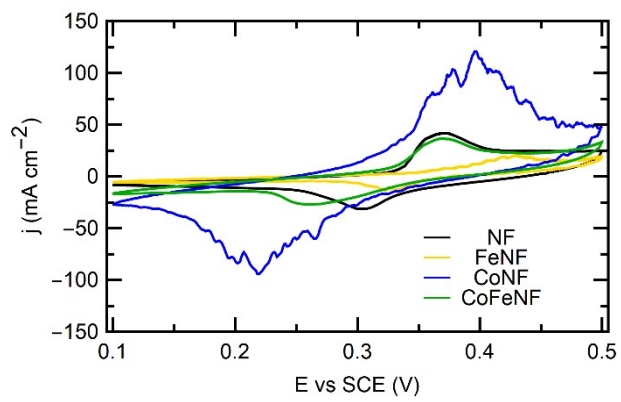


Figure S10. CVs in the non-faradaic region for oxides films deposited from the noted metal ions on nickel foam, at  $100 \text{ mV s}^{-1}$

Structure	Catalyst	Method	Electrolyte	Substrate	Overpotential $\eta_{10}$ (mV)	Tafel slope (mV dec <sup>-1</sup> )	Reference
Amorphous	CoO <sub>x</sub>	ORR driven deposition	1 M KOH	RVC	316		This work
Amorphous	NiO <sub>x</sub>	ORR driven deposition	1 M KOH	GC	330	48	This work
Amorphous	NiO <sub>x</sub> /Ni	Electrodeposition + anodization	1 M KOH	Au	350	42	McCroy et al. 2013.
Amorphous	CoO <sub>x</sub> /Co	Electrodeposition + anodization	1 M KOH	Au	390	70	McCroy et al. 2013.
Amorphous	Co(OH) <sub>2</sub>	Electrodeposition + anodization	1 M KOH	NF	290	91	Wang et al. 2020.
Nanosheets	NiCo <sub>2</sub> O <sub>4</sub>	Nanoparticle deposition	1 M KOH	GC	343	66	Campos-Martin et al., 2006.
Nanosheets	CoMn LDH	Nanoparticle deposition	1 M KOH	GC	312	33	Song et al., 2014.
Nanoparticles	IrO <sub>2</sub>	Nanoparticle deposition	1 M KOH	GC	326	48	Song et al., 2014.

*Table S1 Collection of state of the art landmark materials of Ni, Co, Mn, and Ir for benchmarking the electrocatalytic performance for the oxygen evolution reaction.*

References for Table S1.

C. C. McCrory, S. Jung, J. C. Peters, and T. F. Jaramillo. "Benchmarking heterogeneous electrocatalysts for the oxygen evolution reaction". In: *Journal of the American Chemical Society* 135.45 (2013), pp. 16977–16987.

S. Wang, T. Wang, X. Wang, Q. Deng, J. Yang, Y. Mao, and G. Wang. "Intercalation and elimination of carbonate ions of NiCo layered double hydroxide for enhanced oxygen evolution catalysis". In: *International Journal of Hydrogen Energy* 45.23 (2020), pp. 12629–12640.

J. M. Campos-Martin, G. Blanco-Brieva, and J. L. Fierro. "Hydrogen peroxide synthesis: an outlook beyond the anthraquinone process". In: *Angewandte Chemie International Edition* 45.42 (2006), pp. 6962–6984.

F. Song and X. Hu. "Ultrathin cobalt–manganese layered double hydroxide is an efficient oxygen evolution catalyst". In: *Journal of the American Chemical Society* 136.47 (2014), pp. 16481–16484.



